Chemical Engineering Journal 158 (2010) 520–527

Contents lists available at ScienceDirect

Chemical Engineering Journal

journal homepage: www.elsevier.com/locate/cej

Screening of combined zeolite-ozone system for phenol and COD removal

Nor Aishah Saidina Amin*, Javaid Akhtar, H.K. Rai

Chemical Reaction Engineering Group (CREG), Faculty of Chemical and Natural Resources Engineering, Universiti Teknologi Malaysia, 81310 UTM, Skudai, Johor Darul Takzim, Malaysia

ARTICLE INFO

Article history:
Received 8 November 2009
Received in revised form 19 January 2010
Accepted 20 January 2010

Keywords:
Zeolites
HZSM-5
Phenol
Ozonation
Adsorption

ABSTRACT

In this study, four zeolites in H-form (HZSM-5, H-Beta, H-Mordenite, and H-USY) were tested at different operating conditions for removal of phenol and COD by ozonation. The process variables include concentration of phenol in solution, ozonated airflow rates, pH of solution, temperature, and reaction time. According to experimental results, combination of zeolite and ozone was able to remove both phenol and COD effectively compared to without ozone. Zeolite mainly acted as adsorbent, providing surface for reaction between ozone and phenol. However, the adsorption capacity of zeolites decreased at higher pH due to the formation of OH radicals, which diminished the surface reactions, but enhanced the bulk removal of phenol. Large flow rates of ozonated air and ambient temperature were suitable for removal of both phenol and COD. A maximum of 50.5% phenol was removed by HZSM-5(80) at 100 ppm of phenol concentration. HZSM-5(80) removed both phenol and COD effectively compared to other zeolites at all operating conditions except when phenol concentration was higher at which H-USY was a better catalyst.

© 2010 Elsevier B.V. All rights reserved.

1. Introduction

Phenol is a basic raw material to numerous products such as pesticides, pharmaceuticals, and phenolic resins that reflects its large industrial production. However, phenol is one of the hazardous chemicals listed in EPA guidelines for 129 priority pollutants. It is a toxic, carcinogenic, and non-biodegradable chemical. It adds toxicity in water streams and is harmful to both human and aquatic animals [1,2]. In many countries, the maximum allowable phenol limits in water streams are less than 1 ppm; for instance ~0.5 ppm for Malaysian wastewater [3,4]. Due to strict regulations, considerable research has been conducted to remove phenol from wastewater streams [1–8].

Ozone has emerged as an environmentally safe oxidizer and disinfector in water treatment area. Ozone can oxidize organic and inorganic matter present in wastewater such as phenols, detergents, sulfides, and nitrates [9]. Ozonation can also detoxify harmful chemicals (such as acids, pesticides) and can decolorize dyes and pigments effectively. Ozone inhibits production of carcinogenic byproducts such as trihalomethanes and chloramines as in case of chlorination [10]. The taste and odor of ozonated water are also improved. The ability of ozone to react with substrate by direct and indirect pathways makes it a suitable oxidant for better removal of pollutants. Despite several advantages for using ozone to remove pollutants from water, there are also several disadvantages, which limit its application to water treatment. These may be (i) ozone generation cost, (ii) low ozone solubility in water and (iii) low oxidation rates towards stable organic compounds such as phenols and oxalic acids. At low pollutant concentrations, removal rates are slow which require high ozone dosages. Higher ozone dosages increase cost of ozonation process [11]. Moreover, incomplete ozonation generates secondary pollutants, which sometimes are more harmful than their precursors [10]. One solution to issues (ii) and (iii) can be the addition of solid particles in water, which can concentrate both pollutants and ozone on their surfaces. Selection of suitable solid may serve two purposes (i) both species are able to concentrate and react faster on the said surface [12], (ii) addition of high ozone dosages is not necessary. It is also suggested that heterogeneous material should not add impurities into the water itself [12].

Previous reports have indicated that high silica zeolites (HSZ) could adsorb sufficient amount of ozone [12,13]. Moreover, these materials have also been applied as adsorbents and catalysts for pollution abatements [7–8,14–15] due to their texture, which includes porosity, extended surface area, and regeneration capability. The hydrophobic nature of HSZ also attracts organic compounds on its surfaces [16] that result in enhanced reaction rates among pollutants and ozone on these concentrated zones [13].

In this study, four different zeolites (HZSM-5, H-β, H-USY, and H-Mordenite) were considered in order to compare their capability to assist removal of aqueous phenol and COD from water during

* Corresponding author. Tel.: +60 7 5535588; fax: +60 7 5581463.
E-mail address: noraishah@fkkksa.utm.my (N.A.S. Amin).

1385-8947/$ – see front matter © 2010 Elsevier B.V. All rights reserved.
doi:10.1016/j.cej.2010.01.042

Nomenclature

$[COD]_0$	initial COD concentration
$[COD]_t$	COD concentration at time t
$[Phenol]_0$	initial phenol concentration
$[Phenol]_t$	phenol concentration at time t
AOP_s	advanced oxidation processes
COD	chemical oxygen demand
KI	potassium iodide
w/w	weight/weight
HZS	high silica zeolites

ozonation process. The cationic form of the zeolites was standardized while the SiO_2/Al_2O_3 ratios were kept similar except the ratio for HZSM-5. The purpose of the study was to screen a suitable zeolite catalyst and operating conditions for removal of phenol by ozonation and to elucidate factors that influence catalyst selection. Efficiencies were compared in terms of percentage of phenol and COD removal.

2. Experimental

2.1. Chemicals

Phenol (phenol solution 80%, w/w, in water) was obtained from BDH Chemicals, England. Buffer solution with ratio of 4 (citric acid), 7 (phosphate) and 10 (boric acid) from Merck were used to adjust the pH of solution. Zeolites namely (i) ZSM-5(30), (ii) Ammo-ZSM-5(80), (iii) Ammo-Beta, (iv) Ammo-Mordenite, and (v) USY were supplied by Zeolyst International, USA. All of the zeolites were either in NH_4^+ (Ammo) or anion form. The SiO_2/Al_2O_3 ratios for all zeolites and supplier specified surface areas are tabulated in Table 1.

2.2. Preparation of zeolites

The ZSM-5 zeolites were calcined at 550 °C for four hours and the Ammo-Beta was calcined at 450 °C for six hours. Meanwhile both the Ammo-Mordenite and USY zeolites were calcined at 500 °C for five hours. High calcination temperatures helped to create the H-form (hydrogen form) of zeolites by decomposing the NH_4-form and removed the organic impurities. Thus, calcinations at the above stated temperatures were enough to convert all the zeolites into H-form [17]. After calcinations, the zeolites were characterized by nitrogen absorption (NA) conducted at the Petronas Research and Scientific Laboratories (PRSS), Bangi, Malaysia. The particle size of all the zeolites was <100 μm. XRD analysis was conducted using a Siemens D5000 employing the Cu Kα technique (λ = 1.51056 Å) with 2θ ranging from 2° to 50°. The scanning speed applied in this analysis was 0.05°/s. FT-IR analysis was also performed on a Shimadzu FT-IR 8000 series using KBr Pellet technique according to the procedure described in [18].

2.3. Ozonation of phenol

Several experiments were performed to test the effectiveness of zeolites for removal of phenol and COD at various operating parameters. The different parameters studied in these experiments were phenol concentrations (ppm) ozonated airflow rates (L/min), temperature (°C) and pH of solution. CODs of phenols solutions were within range of 300 ± 10 to 8250 ± 100 ppm corresponding to 100–3340 ppm concentration of phenol solutions, respectively. Ozone was produced from purified air using ozone generator (Triogen 2B Lab Ozone Generator). The ozonated air (4.0 g O_3/L) produced by ozone generator was dispersed through a semi continuous reactor (500 mL glass bottle) containing 350 mL of phenol solution and 1.0 g of powdered zeolite. The reactor was continuously stirred by a magnetic stirrer (400 rpm) for 20–60 min. The loss of phenol through evaporation was presumed negligible since the volatility of phenol was considerably low. Saturated $Ca(OH)_2$ was used to test CO_2 presence while 2% potassium iodide (KI) solution was used to trap surplus ozone. The percentage of phenol and COD removal was determined by Eqs. (1) and (2), respectively.

$$\%\text{phenol removal} = \frac{[\text{Phenol}]_0 - [\text{Phenol}]_t}{[\text{Phenol}]_0} \times 100 \quad (1)$$

$$\%\text{COD removal} = \frac{[\text{COD}]_0 - [\text{COD}]_t}{[\text{COD}]_0} \times 100 \quad (2)$$

where $[Phenol]_0$ and $[Phenol]_t$ represent initial and instantaneous (at time t) phenol concentrations (ppm), respectively. Similarly, $[COD]_0$ and $[COD]_t$ represent initial and instantaneous (at time t) concentrations of COD in ppm.

2.4. Phenol adsorption test

The adsorption of phenol on zeolite surface was analyzed using the method adapted from elsewhere [19]. An amount of 2.86 g zeolite was added in a stirred glass bottle containing 100 mL of the phenol solution for 30–60 min. The samples were then filtered prior to analysis.

2.5. Analytical procedures

After ozonation, the phenol concentrations were measured using High Performance Liquid Chromatography (HPLC) equipped with Waters 486 UV detector (Agilent, USA). The column used was a reversed phase SGE Wakosil-II 5 μm (15 cm × 0.46 cm). A HPLC grade mixture (40% acetonitrile and 60% water) was chosen as an optimal mobile phase for phenol. The wavelength of the UV absorbance used was 254 nm. The COD analysis was carried out with Hach low range reagents (0–150 mg/L) and measured using a Hach DR2000 spectrophotometer.

Table 1
Surface area and pore dimensions of zeolites.

Zeolite	SiO_2/Al_2O_3	Supplier's specification	After calcination	
		Surface area (m^2/g)	Surface area (m^2/g)	Pore dimension (nm)
HZSM-5(30)	30	400	353	0.53 × 0.56 and 0.51 × 0.55
HZSM-5(80)	80	351	339	0.53 × 0.56 and 0.51 × 0.55
H-Beta	25	680	501	0.65 × 0.56 and 0.75 × 0.57
H-Mordenite	20	500	481	0.65 × 0.70 and 0.26 × 0.57
H-USY	30	780	743	0.74 × 0.74

3. Results and discussion

3.1. Characterization of zeolites

The surface areas of the zeolites (Table 1) measured by N_2 adsorptions are in the following order: H-USY > H-Beta > H-Mordenite > HZSM-5(80) > HZSM-5(30). The surface areas of the calcined zeolites were lower than their original NH_4^+ or anion forms. The percentage reduction in the surface areas in H-form zeolites were 26.2% (H-Beta), 12% (HZSM-30), 9.4% (HZSM-80), 4.7% (H-USY), and 3.8% (H-Mordenite). Since the crystallite structures of zeolites possess more pore volume and larger surface area than their amorphous forms, it is clear that disintegration had occurred in crystal lattices of the calcined zeolites to some extent, although the crystallinity of zeolites was not much disturbed by calcinations except in H-USY. The pore size depends on the number of atoms in the ring structure of zeolite. H-Beta and H-USY zeolites have large pore size due to the presence of 12-membered oxygen ring structure in its crystal lattice, while H-form ZSM-5 has medium pore size (10-membered oxygen ring). Pore dimensions have some direct relationship with surface area of zeolites as shown in Table 1, where the surface area is higher for zeolites having larger pore dimensions. However, higher SiO_2/Al_2O_3 contents may increase the surface area [20], as calcined sample of ZSM-5(80) had larger surface area than ZSM-5(30) even at similar pore dimensions.

Fig. 1 shows the XRD patterns for calcined HZSM-5, H-Beta, H-Mordenite, and H-USY zeolites. The peaks for HZSM-5 were similar to those of Tan et al. [21], indicating that there was no significant reduction in crystallinity at around 550 °C. Moreover, H-Beta, H-Mordenite, and H-USY were also in well crystalline form when compared with the literature data [22]. The FT-IR spectra for calcined zeolite samples for the spectral range 1400–400 cm^{-1} is displayed in Fig. 2.

The HZSM-5 zeolite exhibited similar spectral peaks as that of uncalcined ZSM-5 sample [23], which suggests that the crystalline structure of HZSM-5 was still intact. However, the spectral peaks in HZSM-5 were not as sharp as in uncalcined ZSM-5 possibly suggesting that the degree of crystallinity was lower in calcined sample than that of uncalcined ZSM-5. Moreover, none of the calcined samples exhibited spectral peak for ammonium ion at 1398–1400 cm^{-1} suggesting that hydrogen ions has replaced NH_4^+ ions from the zeolite samples during calcinations [18]. Thus, H-form zeolites had both less crystallinity and surface area than their original NH_4^+ or anion forms.

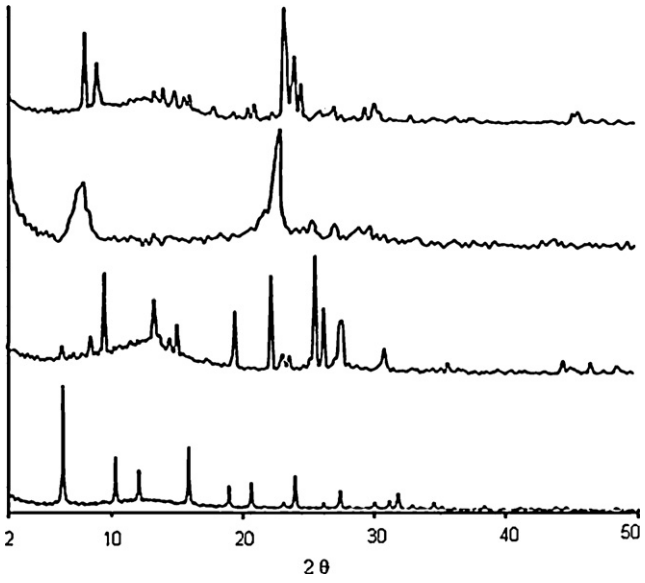

Fig. 1. X-ray diffraction patterns of (a) HZSM-5 (b) H-Beta (c) H-Mordenite and (d) H-USY.

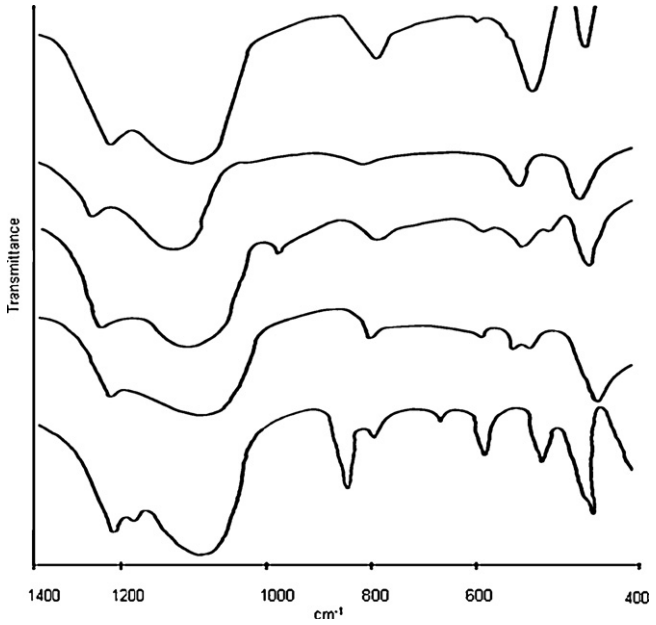

Fig. 2. FT-IR spectra of (a) HZSM-5 (30), (b) HZSM-5 (80), (c) H-Beta, (d) H-Mordenite and (e) H-USY.

3.2. Adsorption of phenol on zeolite surface

The phenol adsorption capability of calcined zeolites for initial concentrations of phenol at 100 and 3400 ppm is exhibited in Fig. 3. Phenol adsorption was negligible in H-Mordenite. For 100 ppm, HZSM-5(80) and H-Beta adsorbed more phenol on their surfaces adsorbing 40% and 30% of initial phenol concentration, respectively. However, phenol adsorption was higher in H-USY than that of HZSM-5(80) or H-Beta at 3400 ppm of initial phenol concentration.

Properties such as pore dimensions, surface area, SiO_2/Al_2O_3 ratio, hydrophilic and hydrophobic character modify the competitive adsorption of phenol or water on zeolites surfaces [12,24]. Silica contents add hydrophobic character to the zeolite catalysts. In general, hydrophobic zeolites have more affinity towards organic compounds such as phenol compared to hydrophilic ones. High silica contents (SiO_2/Al_2O_3 = 80) in HZSM-5(80) led to the effective phenol adsorption at low phenol concentrations [25].

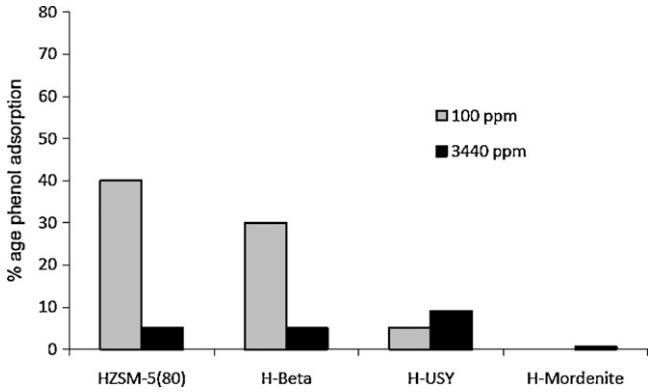

Fig. 3. Adsorption of phenol by different zeolites at 100 ppm and 3440 ppm phenol concentration. *Conditions*: Temperature = 30 °C, stirring speed 400 rpm, reaction time = 30 min.

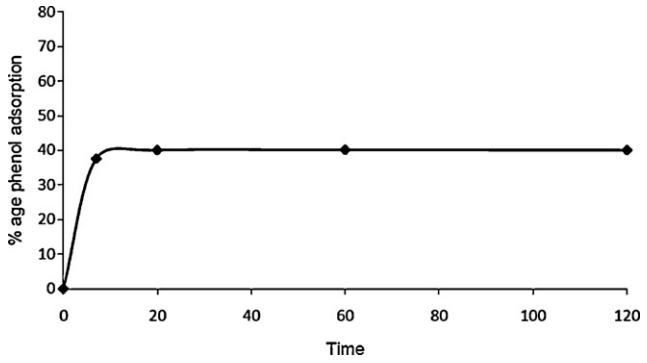

Fig. 4. Profile of phenol adsorption by HZSM-5 (80). *Conditions*: Initial phenol concentration = 100 ppm, reaction time = 30 °C, stirring speed = 400 rpm.

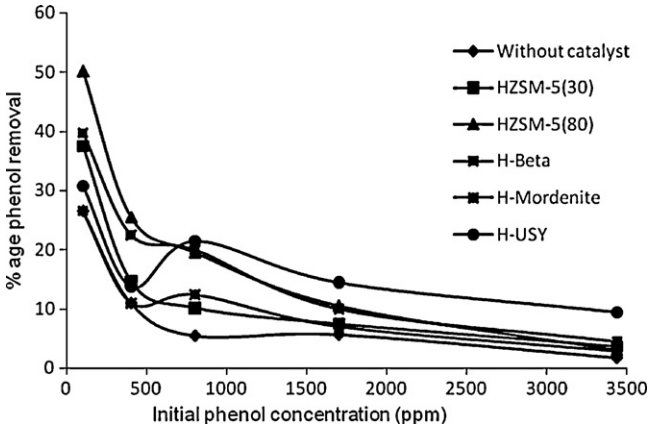

Fig. 5. Influence of initial phenol concentrations on (a) phenol and (b) COD removal. *Conditions*: 30 °C, ozonated airflow rate = 1.0 L/min, reaction time = 15 min.

However, pore dimensions and surface area were two other factors that influenced the phenol adsorption on zeolites. For example, slightly low SiO_2/Al_2O_3 ratio could not halt phenol adsorption in H-Beta due to larger pore dimensions and exposed area. Pore dimensions correspond to the pore volume of porous zeolites. The larger the pore volume, the more will be the probability of phenol adsorption. Moreover, hydrophilic character led to poor phenol adsorption as evident in H-USY, which has low SiO_2/Al_2O_3 ratio and large pore dimensions. Finally, the poorest adsorption capability of H-Mordenite is possibly due to its hydrophilic nature and low SiO_2/Al_2O_3 ratio. Smaller ring dimension (0.26 nm × 0.57 nm) was another reason for poor phenol adsorption in H-Mordenite since the molecular size of phenol is 0.6 nm [6]. Moreover, due to mono-dimensional pore structure in H-Mordenite, the first phenol molecule adsorb on the mouth of pore possibly limits the diffusion of other molecules resulting in the reduction in overall adsorption of phenol.

At higher concentrations, the probability of phenol adsorption on zeolite surface is higher than that of water. At such concentrations, the pore volume becomes a prominent factor than SiO_2/Al_2O_3 ratio or hydrophobic nature. Due to the same reasons, adsorption was the highest in the porous H-USY zeolite. This was also true for H-Mordenite, where adsorption of phenol was enhanced at high concentrations of phenol. High SiO_2/Al_2O_3 ratio could not help much to adsorb phenol on HZSM-5(80). The overall adsorption percentage was low for higher phenol concentrations compared to that at low concentrations. After the saturation level is reached, it was not possible for any extra amount of phenol to adsorb even after 120 min. Fig. 4 illustrates the adsorption of phenol on HZSM-5 surface at 100 ppm initial phenol concentration. Adsorption of phenol reached its saturation during the first 20 min. The purpose of this graph was to identify the effect of adsorption on phenol removal. As discussed later in Fig. 9, the rate of phenol removal was high during the first 20 min of ozonation but reduced afterwards. This suggested the adsorption capability of zeolite was one major factor for phenol removal.

Conclusively, several factors influenced the adsorption of phenol on zeolite surface such as the nature of zeolites (hydrophilic/hydrophobic), surface area, pore size, SiO_2/Al_2O_3 ratio, and aqueous concentration of phenol. At low phenol concentrations, hydrophobic surface was the better adsorbent [6]. At high phenol concentration, surface area and pore volume of the adsorbent were dominant parameters due to high collision and diffusion of phenol molecules.

3.3. Removal of phenol and COD

The color of the saturated $Ca(OH)_2$ solution turned cloudy in all experimental runs indicating the presence of carbon dioxide in the outlet of the ozonation reactor. The color change suggested that phenol was mineralized to CO_2 by passing ozonated air through phenol solution. In addition, the time of ozone appearance in the exit gas (indicated by color change of the KI solution from clear to yellowish) ranged from few seconds to minutes. The time delay in the color changes of KI solution during catalyzed ozonation compared to without catalyst ozonation, indicated the possibility of efficient ozone utilization in the zeolites/ozone system [19]. The following subsections describe the effect of different parameters on removal of phenol.

3.4. Effect of initial concentration

Fig. 5 shows the effect of initial concentration of phenol on removal capability of zeolites.

At 100 ppm of initial concentration, the order of zeolites for percentage removal of phenol was HZSM-5(80) > HZSM-5(30) > H-Beta > H-Mordenite, similar to that observed for adsorption of phenol inferring that adsorption was supportive to ozonation process. Moreover, as ozone itself degraded sufficient amount of phenol in the absence of any zeolite, it also highlighted that bulk reactions among ozone and phenol were also significant. The zeolites mainly acted as an adsorbent and to lesser extent as a facilitator for ozone/phenol reactions. At 100 ppm of initial phenol concentrations, the %age removal of phenol was higher in all zeolite cases compared to that at 3340 ppm. Removal capability shrank sharply to <5% at 3400 ppm of initial concentrations for all of the zeolites except for H-USY (9.5% phenol removal). This was mainly due to the insufficient supply of ozone to handle such high concentrations of phenol [19]. However, it is notable that the increase in initial concentration of the phenol supported the removal performance of both catalytic and non-catalytic cases. For example, H-USY removed 279 mg of more phenol at 3340 ppm compared to that at 100 ppm. Similarly, H-Beta removed 56 mg of more phenol at 3340 ppm. Although, HZSM-5(80) was effective to remove phenol at low concentrations, H-USY and H-Beta removed more phenols at high concentrations (Fig. 5). Moreover, increasing initial phenol concentration enhanced phenol removal even in the absence of any zeolite, suggesting the enhancement in bulk reactions at higher phenol concentrations. This enhancement in ozone consumption is due to high concentration of organic matter as observed in [26]. H-USY and H-Beta showed better removal capability at higher phenol concentrations possibly due to their large pore dimensions and exposed areas. For 500–800 ppm initial phenol concentration, the sudden increase in phenol removal in the case of H-USY or H-Mordenite shows a shift of dependence of phenol adsorption from SiO_2/Al_2O_3 ratio to pore volume of the zeolite. As shown in

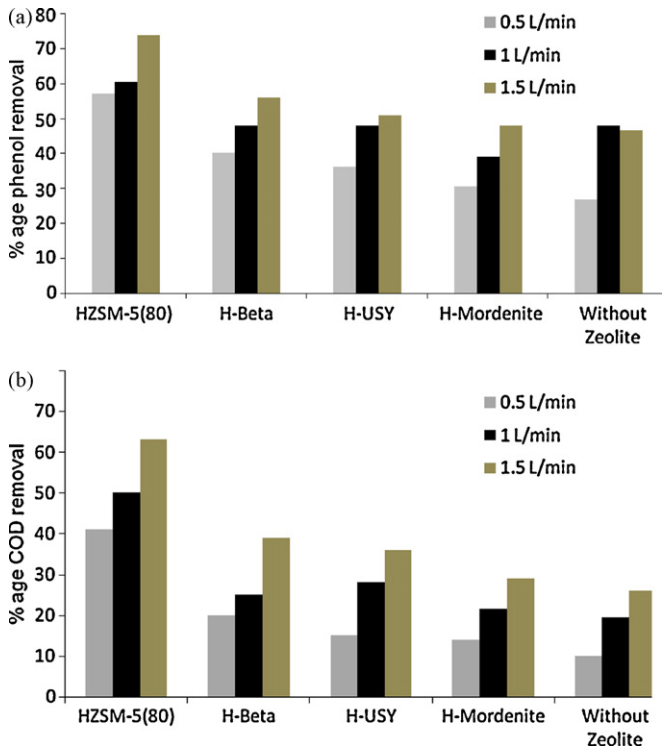

Fig. 6. Influence of ozonated airflow rate (L/min) on (a) phenol and (b) COD removal. *Conditions*: temperature = 30 °C, reaction time = 30 min, initial phenol concentration = 100 ppm.

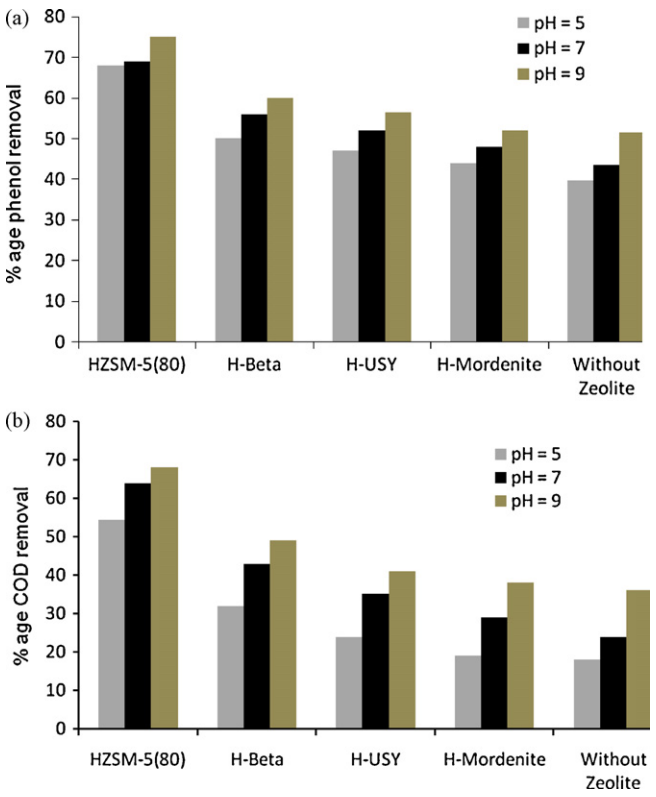

Fig. 7. Influence of initial pH of solution on (a) phenol and (b) COD removal. *Conditions*: Temperature = 30 °C, initial phenol concentration = 100 ppm, ozonated airflow rates = 1.0 L/min, reaction time = 60 min.

Fig. 5, high phenol removal in H-USY after a critical concentration at 800 ppm is mainly owed to the high porous volume or surface area of H-USY compared to other zeolites. USY, being three-dimensional porous structure facilitates multidirectional adsorption of phenol molecules that enhances the amount of phenol adsorbed per unit volume of pore annulus unlike in H-Mordenite. As pore size and pore structure becomes dominant factors at high concentration of phenol, the rate of removal of phenol increases in USY due to the presence of multiple pore annuli.

High phenol concentrations minimized the effect of SiO_2/Al_2O_3 ratio or hydrophilic character of zeolites, which made pore volume or pore dimensions as major parameters during ozonation. Enhancement in phenol removal capability in H-USY or H-Beta at higher concentrations was due to their larger pore volume or pore size compared to HZSM-5. The order of performance for the top three zeolites for phenol removal at 3340 ppm was: H-USY, HZSM-5(80), and H-Beta, which highlighted the importance of pore dimensions, surface area, and SiO_2/Al_2O_3 ratio as major parameters.

3.5. Effect of ozonated airflow rates

No further study was conducted at high phenol concentration (3340 ppm) due to low removal of phenol at this concentration. Common phenol concentration reported for ozonation experiments was 100 ppm [27,28]. HZSM-5(30) was also not considered for further experimental tests due to its low performance compared to HZSM-5(80).

Fig. 6(a) shows the effect of ozonated airflow rates on removal of phenol. HZSM-5(80) degraded the maximum amount of phenol at 1.5 L/min of ozonated airflow rates among all of the zeolites while. H-Beta and H-USY followed the order. Phenol removal was negligibly higher in case of H-Mordenite compared to that in the absence of any zeolite. The substantial increase in phenol removal with airflow rates is attributed to the enhancement in the rate of mass transfer from ozone air bubbles to the liquid phase. This owes to (i) enhancement in eddies formation and turbulence of gas bubbles reduced the ozone diffusion limitations across the boundary of bubbles and (ii) increase in gas holdup times (ε) according to Eq. (3) [29], which enhances the probability of ozone diffusion from gas phase to solution.

$$\varepsilon\alpha(\text{gas flow rates})^n \quad (3)$$

where the values of n range from 0.7 to 1.2 for low velocity of bubbling gases. Secondly, ozone concentration has direct relationship with flow rates of ozonated air. Increasing airflow rates through ozone generator increases the overall amount of ozone concentration per unit time (mg/min), which leads to enhancement in diffusion of ozone from gas to solution.

Similar effect of ozonated airflow rates on COD removal is displayed in Fig. 6(b). Low COD removal corresponds to the presence of refractory species, which are probable products of ozonation. This trend is common in many investigations. Ozonation causes fragmentation in phenol compound leading to the formation of stable compounds that are hard to remove. The sequence for COD removal was also similar at all ozonated airflow rates:

HZSM-5(80) > H-Beta > H-USY.

The trend indicates SiO_2/Al_2O_3 ratio is a major parameter at low initial concentrations.

3.6. Effect of pH of solution

The effect of pH of solution, shown in Fig. 7, indicates that pH promoted phenol removal in all zeolite cases. It was notable that increase in pH supported the bulk removal more rather than surface adsorption of phenol; percentage increase in phenol removal was the highest in only ozonation case. The bulk removal was attributed

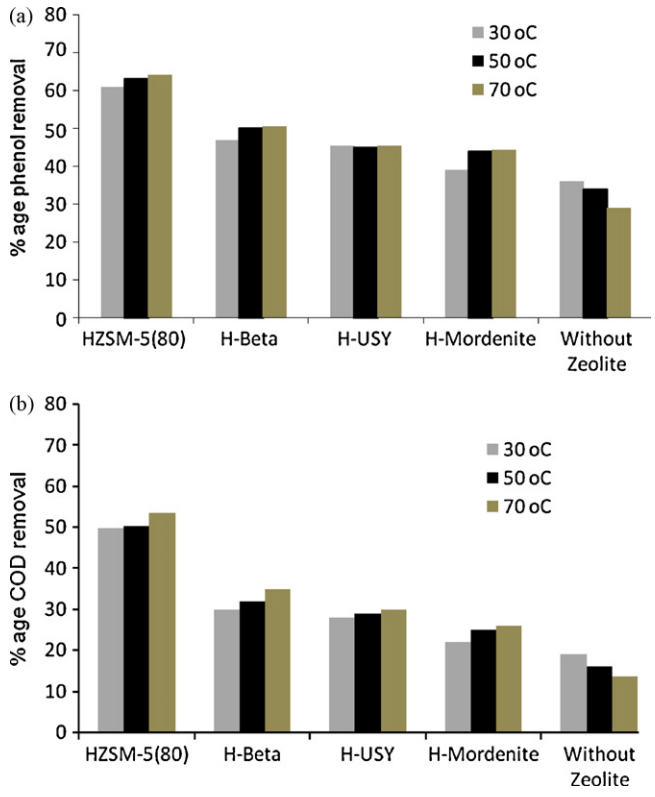

Fig. 8. Influence of temperature (°C) on (a) phenol and (b) COD removal. *Conditions*: Initial phenol concentration = 100 ppm, ozonated airflow rates = 1.0 L/min, reaction time = 30 min.

to the enhancement in the formation of OH radicals, which have greater potential to degrade phenol or its byproducts [30] and decomposed ozone according to Eqs. (4) and (5).

$$O_3 + OH^{-1} \rightarrow HO^{-2} + O_2 \quad (4)$$

$$2O_3 + HO^{-2} \rightarrow OH^{\bullet} + O_2^{\bullet -} + O_2 \quad (5)$$

On the other hand, surface adsorption of phenol decreased at high pH mainly because the basic solution led to the decrease in adsorption capacity of zeolites [24] due to the repulsion of anion forms of phenol solution and negatively charged zeolites. Rather, accumulation of H^+ ions increases on surface of zeolites, which lessens (i) the population of adsorbed OH^{-1} and availability of free sites on the zeolites [31]. Thus, decreasing pH of solution will reduce the capability of zeolites to remove ozone.

The enhancement in phenol removal as observed in our study mainly owes to the decomposition of ozone and direct reactions between phenol and OH radicals. As shown in Fig. 7(b), the removal of COD followed a similar pattern; HZSM-5(80) exhibited the maximum COD removal capability followed by H-Beta > H-USY. COD removal was lower than that of phenol mainly because of the same reasons discussed previously.

3.7. Effect of temperature

Fig. 8 illustrates that the effect of temperature on the phenol and COD removal was insignificant. Percentage increase in phenol removal due to temperature rise were 6.2% (H-Mordenite) > 3.19% (H-Beta) > 2.25% (HZSM-5) > 0.54% (H-USY). COD removal exhibited a similar trend. Ozonation in the absence of any zeolite actually observed 7.42% less phenol removal at 70 °C compared to that of 30 °C, the negative effect of temperature on phenol removal mainly owes to the sharp reduction in ozone dissolution at high temperature [32]. However, high temperature enhances the rate of

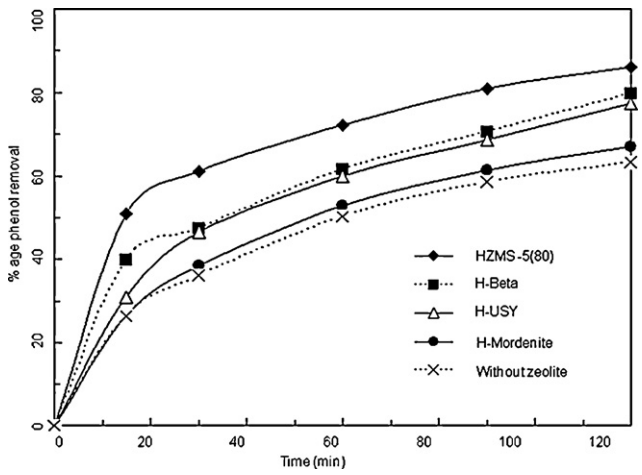

Fig. 9. Profile of (a) phenol and (b) COD removal verses ozonation time. *Conditions*: 100 ppm phenol, temperature = 30 °C, ozonated airflow rate = 1.0 L/min.

reaction among pollutants and ozone at zeolite surface [12] which may explain the small increase in percentage phenol removal as observed in our study. Overall, ambient temperature is recommendable for ozonation studies.

3.8. Effect of reaction time

Fig. 9 shows the degradation behavior of phenol as a function of time at 100 ppm of initial phenol concentration. The first 20 min observed fast removal rates before the onset of secondary slow phase. For instance, out of 86% total phenol removal in HZSM-5(80), 58% was removed in the first 20 min. Zeolites performance order was the same as discussed before; HZSM-5 > H-Beta > H-USY since zeolites mainly acted as adsorbents and the adsorption of phenol on zeolite surface reached its saturation point within the first 20 min (Fig. 4) which indicated the probability of high rates of phenol removal during this time period. Initial concentration of phenol is another factor that determines the rate of reactions. Gradual decrease in initial phenol concentration and appearance of refractory species as ozonation proceeds lead the slowness in the reaction rates.

3.9. Role of zeolite catalyst in phenol ozonation

During ozonation of phenol, zeolite mainly acted as an adsorbent for both ozone gas and phenol. This increased the probability of reactions among ozone and pollutant species. Ozone decomposition at zeolite surface was considerably low except for high pH values. Fujita et al. [12] demonstrated the capability of ZSM-5 for adsorbing high ozone concentrations. Studies have suggested that hydrophobic zeolites can absorb pollutant and oxidant species on their surface to support better interactions [33,34]. The current study resulted in similar consequences (see Figs. 3–5). Thus, it is presumed that adsorption and surface reactions are major pathways for phenol removal on zeolite surfaces as shown in Fig. 10. Secondly, as discussed above, the removal of phenol was also significant in absence of any catalyst highlighting the role of molecular ozone in decomposition of phenol. The bulk decomposition was increased by (i) increasing the concentration of phenol in solution and (ii) at higher pH values. Interactions among phenol and ozone molecules were enhanced at high phenol concentrations that led the enhancement in overall phenol removal. Moreover, the decomposition of ozone in basic medium also helped the removal of phenol in bulk phase. The effect of increase in pH seems conventional during which bulk ozone was decomposed into OH

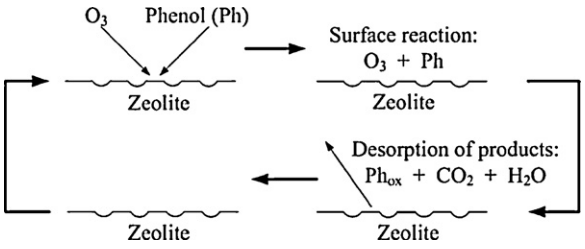

Fig. 10. Mechanism for removal of phenol during zeolite enhanced ozonation.

radicals, which are better oxidants to removal phenol even in bulk phase.

The first possibility of ozone attack on phenol is through O–H bond, which leads to the production of phenol derivatives. The other possibility is the electrophilic addition of ozone on phenol that leads to decomposition of ring structure producing carboxylic acids and open ring alcohol radicals [35,36]. These intermediates decompose further into water or CO_2 only by OH radical decomposition mechanism, since OH radicals have better ability to mineralize relatively stable organic acids. Increase in pH level and bulk reactions among reacting species are two major sources for generation of OH radicals. However, the possibility of mineralization degree remains usually low. The major decomposition products include olefins, organic acids, or phenol derivates [37]. Eq. (6) shows the possible scheme for decomposition of phenol in bulk phase by direct molecular ozone. The schemes for decomposition of phenol through OH radical mechanism are listed in Eqs. (7)–(11) [37].

$$O_3 + C_6H_5\text{–}OH \rightarrow R\text{–}COOH + R\text{–}OH + R\text{–}O^* + OH^* \rightarrow \text{Stable products} \quad (6)$$

$$O_3 \xrightarrow{\text{basic pH}} OH^* \quad (7)$$

$$OH^* + R\text{–}COOH \rightarrow R^* + CO_2 + H_2O \quad (8)$$

$$OH^* + C_6H_5\text{–}OH \rightarrow C_6H_5\text{–}O^- + H_2O \quad (9)$$

$$O_3 + C_6H_5 - O^- \rightarrow C_6H_5 - O^* + O_3^- \rightarrow \text{Stable products} \quad (10)$$

$$H^+ + O_3^- \rightarrow OH^* + O_2 \quad (11)$$

4. Conclusions

The results from catalyst screening indicated higher phenol and COD rejections in all ozone/zeolite systems except for H-Mordenite and without zeolite case. Among all zeolites tested, HZSM-5(80) represented the highest phenol removals for <750 ppm phenol concentrations while H-USY was superior at higher concentrations. However, removal rates were considerably low in concentrated phenol solutions, which required higher oxidant dosages. Moreover, phenol removal was almost independent of temperature variations. Ozonated airflow rates and pH on the other hand considerably contributed to removal rates. Maximum removal of phenol was achieved at pH 9 and 1.5 L/min ozonated airflow rates. The removal rates were faster during first 20 min of operation; gradually decreased afterwards. Nature of adsorbents (hydrophilic/hydrophobic), phenol concentrations, silica/alumina ratio, surface area, and pore size were considered other factors to define suitability of zeolite for decomposition of organics. In this study, HZSM-5(80) was the most promising zeolite for removals of phenols and COD via ozonation.

Acknowledgements

The authors gratefully acknowledge the financial support received in the form of a research grant (Project No.: 08-02-06-004 EA138) from the Ministry of Science, Technology and Innovation (MOSTI), Malaysia.

References

[1] Y.C. Hsu, J.H. Chen, H.C. Yang, Calcium enhanced COD removal for the ozonation of phenol solution, Water Res. 41 (2007) 71–78.
[2] H. Liu, M.Y. Liang, C.S. Liu, Y.X. Gao, J.M. Zhou, Catalytic degradation of phenol in sonolysis by coal ash and H_2O_2/O_3, Chem. Eng. J. 153 (2009) 131–137.
[3] M. Matheswaran, I.S. Moon, Influence parameters in the ozonation of phenol wastewater treatment using bubble column reactor under continuous circulation, J. Ind. Eng. Chem. 15 (2009) 287–292.
[4] A. Idris, K. Saed, Degradation of phenol in wastewater using anolyte produced from electrochemical generation of brine solution, Global Nest Int. J. 4 (2002) 139–144.
[5] T. Lesko, A.J. Colussi, M.R. Hoffmann, Sonochemical decomposition of phenol: evidence for a synergistic effect of ozone and ultrasound for the elimination of total organic carbon from water, Environ. Sci. Technol. 40 (2006) 6818–6823.
[6] N. Roostaei, F.H. Tezel, Removal of phenol from aqueous solutions by adsorption, J. Environ. Manage. 70 (2004) 157–164.
[7] P. Cosoli, M. Ferrone, S. Pricl, M. Fermeglia, Hydrogen sulfide removal from biogass by zeolite adsorption. Part II. M D simulations, Chem. Eng. J. 145 (2008) 93–99.
[8] K.K. Singh, K.D.P. Nigam, Catalytic wet oxidation of phenol in a trickle bed reactor, Chem. Eng. J. 103 (2004) 51–57.
[9] M.A.T. Alsheyab, A.H. Munoz, Optimization of ozone production for water and wastewater treatment, Desalination 217 (2007) 1–7.
[10] W. Wang, B. Ye, L. Yang, Y. Li, Y. Wang, Risk assessment on disinfection by-products of drinking water of different water sources and disinfection processes, Environ. Int. 33 (2007) 219–225.
[11] M. Shiraga, T. Kawabata, D. Li, T. Shishido, K. Komaguchi, T. Sano, K. Takehira, Memory effect-enhanced catalytic ozonation of aqueous phenol and oxalic acid over supported Cu catalysts derived from hydrotalcite, Appl. Clay Sci. 33 (3–4) (2006) 247–259.
[12] H. Fujita, J. Izumi, M. Sagehashi, T. Fujii, A. Sakoda, Adsorption, and decomposition of water dissolved ozone on high silica zeolites, Water Res. 38 (2004) 159–165.
[13] H. Fujita, J. Izumi, M. Sagehashi, T. Fujii, A. Sakoda, Decomposition of trichloroethene on ozone-absorbed high silica zeolites, Water Res. 38 (2004) 166–172.
[14] R. Apiratikul, P. Pavasant, Sorption of Cu^{2+}, Cd^{2+} and Pb^{2+} using modified zeolite from coal fly ash, Chem. Eng. J. 144 (2008) 245–258.
[15] H. Kusic, N. Koprivanac, A.L. Bozic, Minimization of organic pollutant content in aqueous solution by means of AOPs: VU and ozone-based technologies, Chem. Eng. J. 123 (2006) 127–137.
[16] Y. Takeuchi, H. Iwamotob, N. Miyata, S. Asano, M. Haradac, Adsorption of l-butanol and p-xylene vapor and their mixtures with high silica zeolites, Sep. Sci. Technol. 5 (1995) 23–34.
[17] R. Anand, B.S. Rao, Conversion of piperazine over acidic zeolites, Catal. Commun. 3 (2002) 479–486.
[18] N.A.S. Amin, D.D. Anggoro, Dealuminated ZSM-5 zeolite catalyst for ethylene oligomerization to liquid fuels, J. Nat. Gas Chem. 11 (2002) 79–86.
[19] C. Canton, S. Esplugas, J. Casado, Mineralization of phenol in aqueous solution by ozonation using iron or copper salts and light, Appl. Catal. B 43 (2003) 139–149.
[20] L. Shirazi, E. Jamshidi, M.R. Ghasemi, The effect of Si/Al ratio of ZSM-5 zeolite on its morphology, acidity and crystal size, Cryst. Res. Technol. 43 (2008) 1300–1306.
[21] P.L. Tan, Y.L. Leung, S.Y. Lai, C.T. Au, The effect of calcination temperature on the catalytic performance of 2 wt% Mo/HZSM-5 in methane aromatization, Appl. Catal. A 228 (2002) 115–125.
[22] Z. Sun, J. Xu, Z. Du, W. Zhang, Decomposition of cyclohexyl hydroperoxide over transition metal-free zeolite H-beta, Appl. Catal. A 323 (2007) 119–125.
[23] Y. Cheng, L.J. Wang, J.S. Li, Y.C. Yang, X. Yun, Preparation and characterization of nanosized ZSM-5 zeolites in the absence of organic template, Mater. Lett. 59 (2007) 3427–3430.
[24] M. Khalid, G. Joly, A. Renaud, P. Magnoux, Removal of phenol from water by adsorption using zeolites, Ind. Eng. Chem. Res. 43 (2004) 5275–5280.
[25] D.H. Olson, W.O. Haag, W.S. Borghard, Use of water as a probe of zeolitic properties: interaction of water with HZSM-5, Micropor. Mesopor. Mater. 35–36 (2000) 435–446.
[26] C. Cooper, R. Burch, An investigation of catalytic ozonation for the oxidation of halocarbons in drinking water preparation, Water Res. 33 (1999) 3695–3700.
[27] J. Villasenor, P. Reyes, G. Pecchi, Catalytic and photocatalytic of phenol on MnO_2 supported catalysts, Catal. Today 76 (2002) 121–131.
[28] S. Esplugas, J. Gimenez, S. Contreras, E. Pascual, M. Rodriguez, Comparison of different advanced oxidation processes for phenol degradation, Water Res. 36 (2002) 1034–1042.
[29] A.H. Konsowa, Decolorization of wastewater containing direct dye by ozonation in a batch bubble column reactor, Desalination 158 (2003) 233–240.
[30] P.K.A. Hong, Y. Zeng, Degradation of pentachlorophenol by ozonation and biodegradability of intermediates, Water Res. 36 (2002) 4243–4254.
[31] D. Metes, D. Kovacevic, S.P. Vujevic, The role of zeolites in wastewater treatment of printing inks, Water Res. 38 (2004) 3373–3381.

[32] Liquozon, Dissolved ozone delivery subsystem, ozone data and conversion tables, available via http://www.mksinst.com/docs/UR/astexOZONEdata.pdf, retrieved on April 4, 2009.
[33] Y.H. Chen, N.C. Shang, D.C. Hsieh, Decomposition of dimethyl phthalate in an aqueous solution by ozonation with high silica zeolites and UV radiation, J. Hazard. Mater. 157 (2008) 260–268.
[34] J. Farrell, C. Manspeaker, J. Luo, Understanding competitive adsorption of water and trichloroethylene in a high-silica Y zeolite, Micropor. Mesopor. Mater. 59 (2003) 205–214.
[35] S.D. Razumovskii, V.S. Ovechkin, M.L. Konstantinova, The kinetics and mechanism of the reaction of ozone with phenol in aqueous solution, Rus. Chem. Bull. 28 (1979) 261–264.
[36] M.L. Konstantinova, S.D. Razumovskii, G.E. Ziakov, Mechanism of the reaction of ozone with phenols, Rus. Chem. Bull. 40 (1991) 271–275.
[37] M.L. Konstantinova, S.D. Razumovskii, G.E. Ziakov, Kinetics and mechanism of the reaction of ozone with phenols in alkaline media, Rus. Chem. Bull. 40 (1991) 267–270.